Dynamics of Composition Fluctuations in Diblock Copolymer Melts above the Ordering Transition

S. Vogt,† S. H. Anastasiadis,*,‡,§ G. Fytas,*,‡ and E. W. Fischer†

Max-Planck-Institut für Polymerforschung, P.O. Box 3148, 55021 Mainz, Germany, and Foundation for Research and Technology—Hellas, Institute of Electronic Structure and Laser, P.O. Box 1527, 71110 Heraklion, Crete, Greece

Received March 11, 1994; Revised Manuscript Received May 4, 1994●

ABSTRACT: The synthesis of poly(ethylmethylsiloxane-*block*-dimethylsiloxane), EM, copolymers with two blocks that possess similar segmental mobilities, low glass transition temperatures, negligibly small optical anisotropies, but sufficiently different refractive indices was performed in order to study the dynamics of composition fluctuations in disordered diblock copolymer melts. Photon correlation spectroscopy was employed to measure the composition correlation functions $C(q,t)$ for six EM samples with total degree of polymerization N between 240 and 1200 at different wave vectors q and temperatures. For all samples but the one with the lowest N, $C(q,t)$ was found to display two distinct relaxation processes with characteristic pertinent features, in addition to the long range density fluctuations. For the fast relaxation mode, the q-independent relaxation decay rate Γ_1 varies with N^{-3}, whereas the N-dependent amplitude $S_1(q)$ exhibits a q^2 dependence. In the low q limit, the predictions of the random phase approximation for the internal relaxation of the copolymer chain conform well to these experimental findings and, moreover, account almost quantitatively for the values of Γ_1 and $S_1(q)$ of the symmetric EM's. The second relaxation process has a diffusive (q^2-dependent rate) character with q-independent amplitude $S_2(q)$ and its diffusion coefficient, D, agrees well with the self diffusion of the copolymer chain either derived by shear viscosity data or measured by pulsed-field gradient NMR. This second process can be attributed to additional concentration fluctuations due to the inherent composition polydispersity, and, hence, $S_2(q)$ is a measure of its degree, whereas D is the mutual diffusion coefficient. In the EM samples, the latter is predicted and found to be very similar to the self-diffusion coefficient.

I. Introduction

The rich variety of dynamic behavior of block copolymers is currently a subject of intensive research.[1] The link of two chemically dissimilar subchains of N_A and N_B monomers of type A and B, respectively, to form a single copolymer chain A–B leads to a rich phase diagram with characteristic feature the disorder-to-order transition,[2] ODT, from a disordered state to an ordered microphase with decreasing temperature or increasing N ($=N_A+N_B$). In the ordered state, A–B copolymers exhibit self-assembling properties, leading to various long-range ordered microstructures,[2,3] depending on the composition $f = N_A/N$. The equilibrium phase morphology of an A–B melt depends on the product χN, with χ being the Flory–Huggins segment–segment interaction parameter. For a symmetric system, $N_A = N_B = N/2$ and $f = 0.5$, the microscopic ODT for the diblock would set in when $\chi(N_A + N_B) \cong O(10)$, whereas the macroscopic phase separation in a binary polymer blend A/B would occur when $\chi N_A = \chi N_B = 2$. In this χN range, the A and B blocks of the copolymer tend to increase the distance between their centers of mass[4] and develop orientational short-range order[5,6] leading to an excess depolarized light scattering.[5]

For disordered diblocks, the composition fluctuations, expressed in terms of the order parameter $\psi(r,t) = \varphi(r,t) - f$, with $\varphi(r,t)$ being the local volume fraction of A, define the main dynamic variable of the system and their amplitude $\langle\psi_q\psi_{-q}\rangle$ determines the static structure factor $S(q)$ in the wave vector q space. In contrast to the situation in binary blends, the most important $\langle|\psi_q|^2\rangle$ in diblock copolymers has wavelength $\lambda^* \cong O(R_g)$ comparable to the size of the copolymer chain,[2,7,8] where $R_g = (Nb^2/6)^{1/2}$ is the diblock radius of gyration and b the statistical segment length, and, hence, microphase separation takes place at finite wave vectors. The dynamic random phase approximation[9] and the Edwards Hamiltonian approach[10] have been used to derive the dynamic structure factor $S(q,t) = \langle\psi_q(t)\,\psi_{-q}(0)\rangle$ for homogeneous diblock copolymers, which is predicted to relax with a single relaxation process. This relaxation mode is attributed to the relative thermal motion of the two blocks that leads to local composition fluctuations in A–B copolymer melts. The thermal decay rate of this internal relaxation is q independent at low q's, i.e., for $qR_g < 1$, in contrast to the interdiffusion in polymer blends.[11] Moreover, at low q's the intensity associated with the internal relaxation is expectedly quite low, i.e. $S(q) \propto (qR_g)^2$ and, hence, experimental verification utilizing dynamic light scattering requires large N. The internal mode has been experimentally observed recently in A–B solutions[12,13] and, very recently, in A–B melts.[14] In the latter case, photon correlation spectroscopy (PCS) has revealed an additional diffusive (q^2-dependent) process[13–15] that had not been predicted theoretically until recently.[13,16]

In this paper, we have extended the PCS study reported in a recent letter[14] with the main objective to identify the important issues of $S(q,t)$ for A–B disordered melts. The synthesis of poly(ethylmethylsiloxane-*block*-dimethylsiloxane), EM, copolymers consisting of two chemically similar blocks with low χ, composition independent low glass transition temperature T_g, and negligibly small optical segmental anisotropy has facilitated the present study. The EM block copolymer appears to be a model system in the sense that the disordered state can be achieved even for high N's, glass transition effects are not very important, and individual local friction coefficients are comparable so that comparison between experimental results and theoretical predictions becomes less ambiguous.

This article is arranged as follows: In the theoretical background section II, the theoretical predictions on block

* Authors to whom correspondence should be addressed.
† Max-Planck-Institut für Polymerforschung.
‡ Institute of Electronic Structure and Laser.
§ Also at University of Crete, Department of Physics, 711 10 Heraklion Crete, Greece.
● Abstract published in *Advance ACS Abstracts*, June 1, 1994.

0024-9297/94/2227-4335$04.50/0

copolymer dynamics will be reviewed. Following the Experimental Section (section III), the results for the relaxation of composition fluctuations in disordered diblocks are presented in section IV and are discussed in relation to the theoretical predictions in section V. The concluding remarks constitute section VI.

II. Theoretical Background

For bulk homogeneous monodisperse diblock copolymers, the dynamic structure factor $S(q,t) \equiv \langle \psi_q(t)\, \psi_{-q}(0) \rangle$ predicted by the random phase approximation (RPA) is given by[9,12]

$$S_1(q,t) = S_1(q) \exp[-\Gamma(q)t] \tag{1}$$

where ψ_q is the Fourier transform of the order parameter, $\psi(\mathbf{r},t) = \varphi(\mathbf{r},t) - f$. In Leibler's mean field approach,[7] the static structure $S(q)$ assumes the form

$$S_1(q) = \frac{N\upsilon}{F(x,f) - 2\chi N} \tag{2}$$

where $F(x,f)$ is a function of Debye intramolecular correlation functions of Gaussian blocks, $x \equiv q^2R_g^2$ and υ is the average volume per link. Equation 2 has a Lorentzian line shape peaked at $x^*(f) = (q^*R_g)^2 = [3/f(1-f)]^{1/2}$. Inclusion of fluctuation corrections[8] into the mean field approach led to $S(q)$ that still retains the form of eq 2 by replacing χ with an effective interaction parameter χ_{eff}

$$\chi_{eff}N = \chi N - \frac{C(f)}{2\bar{N}^{1/2}}[F(x^*,f) - 2\chi_{eff}N]^{-1/2} \tag{3}$$

where $C(f)$ is a composition dependent coefficient, $\bar{N}$ is a Ginsburg parameter defined by $\bar{N} = Nb^6/\upsilon^2$. In contrast to eq 2 with $S(q)$ diverging at the stability limit $F(x^*,f) - 2\chi_sN = 0$, the peak intensity now attains a maximum $S_1(q^*) = N\upsilon/[F(x^*,f) - 2\chi_{eff}N]$.

The thermal decay rate $\Gamma(q)$ of the composition fluctuations can be written in the form[9,17]

$$\Gamma(x) = \frac{N\,x\,g(1,x)}{2\,\tau\,S(q)} \tag{4}$$

where $g(1,x) \equiv 2[x + \exp(-x) - 1]/x^2$ is the Debye function. For Rouse chains, $\tau = \tau_R = \tau_0N^2/[12f(1-f)]$, with $\tau_0 = \zeta_0b^2/k_BT$ being the microscopic relaxation time, k_B the Boltzmann's constant, and ζ_0 the effective monomeric friction. For entangled chain, $\tau = (5N/4N_e)\tau_R$, where N_e is the number of segments between entanglements.[18] At low x values, i.e., $qR_g < 1$, the thermal decay rate of eq 4 becomes q independent since in the disordered state $N/S(q) \to 3/[2f^2(1-f)^2x]$ and $g(1,x) \to 1$ as $x \to 0$. In this limit, the intensity associated with this internal relaxation is, in principle, low and becomes q^2 dependent. Moreover for Gaussian coils

$$S_1(q) \cong \upsilon f^2 (1-f)^2 N^2 b^2 q^2/9 \quad \text{for } x \ll 1 \tag{5}$$

the scattering intensity is proportional to N^2 and virtually independent of the thermodynamic interactions, i.e., χ. Verification of the validity of eqs 4 and 5 by photon correlation spectroscopy would require high molecular weight copolymers in the homogeneous state possessing a glass transition temperature that is insensitive to composition and N variations. According to eq 4, the thermal decay rate of the composition fluctuations becomes q dependent at intermediate x values and exhibits thermodynamic slowing down behavior near the ODT temperature and $x \cong x^*$. The latter effect has experimentally been observed in binary polymer blends.[11,19]

In the RPA calculations, the internal mode is the only relaxation process for the composition fluctuations in monodisperse A–B copolymers relaxing via relative translational motion of the two blocks. The existence, however, of an additional diffusive relaxation mode (q^2-dependent relaxation rate) experimentally observed in three diblock copolymer melts[14,15,20] and solutions[13] has not been predicted by the dynamic RPA theory. The origin of this new mode can be rationalized in terms of composition polydispersity effects inherent in all real A–B copolymer systems.[13,16,20] Additional concentration fluctuations due to polydispersity can lead to significant scattering at low scattering wave vectors in analogy to the situation in polymer blends. The dynamic structure factor $S_2(q,t)$ associated with the relaxation of these concentration fluctuations in an interacting system is[13,15] for low wave vectors

$$S_2(q,t) = S_2(q) \exp(-Dq^2\,t) \tag{6}$$

with the associated intensity

$$S_2(q) = \frac{N\varkappa_0\upsilon}{1 - 2\,\chi\,N\,\varkappa_0} \tag{7}$$

and diffusion coefficient

$$D = D_s(N)\,(1 - 2\chi N\varkappa_0) \tag{8}$$

As expected, eqs 7 and 8 are reminiscent of the static structure factor $S(0) = N\varphi_A\varphi_B/[1 - 2\chi N\varphi_A\varphi_B]$ and interdiffusion $D_{int} = D_s(1 - 2\chi N\varphi_A\varphi_B)$ in unentangled polymer blends, where the variance of the block copolymer composition[13,15] $\varkappa_0 \cong 2\delta f^2(1-f)^2/[f^2 + (1-f)^2]$, with $\delta = N_w/N_n - 1$, stands for the product $\varphi_A\varphi_B$. Thus, this diffusive mode cannot be detected for monodisperse A–B copolymers and, therefore, was not considered by the RPA theory earlier. The diffusion constant D is essentially the self diffusion D_s of the copolymer chain in the disordered state and is a function of the molecular weight; for Rouse chains,

$$D_s(N) = k_BT/(\zeta_0N) \tag{9a}$$

whereas in the entangled regime

$$D_s(N) = 4k_BT\,N_e/(15\zeta_0N^2) \tag{9b}$$

In the context of this model, it is the presence of nonzero $\varkappa_0$ in addition to the difference in the refractive indices of the block components that allows the measurement of the self-diffusion by dynamic light scattering in an "one"-component system. Inspection of eqs 1–5 and eqs 6–8 reveals pertinent disparities between the two composition-relaxation modes with regard the effect of N and q. Experimental documentation would promote the understanding of the diblock copolymer dynamics.

III. Experimental Section

Materials. Diblock copolymers of polyethylmethylsiloxane (PEMS) and polydimethyl-siloxane (PDMS) were synthesized via anionic polymerization of the cyclic trimers. The cyclic trimer of ethylmethylsiloxane was prepared by condensation of dichloroethylmethylsilane by zinc oxide,[21] whereas the hexamethylcyclotrisiloxane was obtained through thermal cracking of PDMS.[22] The polymerization was carried out using a high-vacuum technique[23] to ensure the full exclusion of air and moisture. First, a small fraction of a prescribed amount of 1,3,5-

Table 1. Molecular Characteristics of the Poly(ethylmethylsiloxane-*block*-dimethylsiloxane) Diblocks

sample	w_E[a]	M_n	M_w/M_n	N_w	T_g	ODT (K)	χN at 80 °C
EM-1	0.54	20 000	1.08	240	140±9	-	1.5
EM-2	0.50	45 000	1.04	580	144±15	<200	3.5
EM-3	0.48	68 000	1.12	890	137,147	252	5.5
EM-4	0.49	95 000	1.04	1200	138,147	298	7.5
EM-5	0.69	67 000	1.05	840	139,148	251	4.9
EM-6	0.37	67 000	1.03	880	140,150	253	5.2

[a] Weight fraction of polyethylmethylsiloxane block, PEMS.

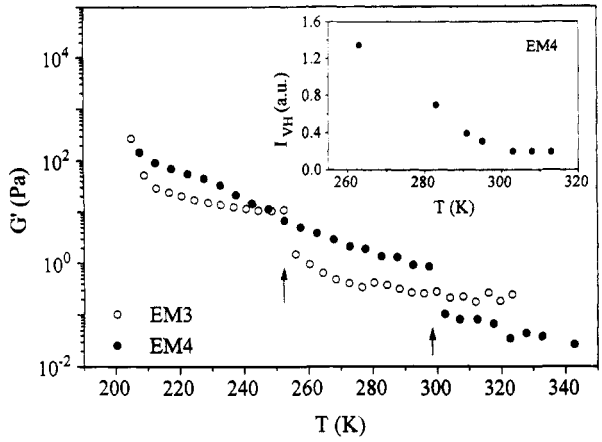

Figure 1. Variation of storage shear modulus G' at frequency 1 rad/s with temperature for poly(ethylmethylsiloxane-*block*-dimethylsiloxane), EM, copolymers: (○) EM-3 and (●) EM-4. The arrows at the discontinuities of $G'(T)$ determine the ODT. The latter can also be estimated by depolarized light scattering intensity measurements shown for EM-4 in the inset.

triethyl-1,3,5-trimethylcyclotrisiloxane was reacted in dry tetrahydrofuran (THF) with *n*-butyllithium as initiator for several hours. The remaining trimer dissolved in THF was then introduced and allowed to polymerize at room temperature for 70 h. Characterization of small samples of the precursor polyethylmethylsiloxane by gel permeation chromatography (GPC) reveals its narrow molecular weight distribution (M_w/M_n = 1.03–1.05). After completion of the first step, the polymer solution was diluted with dry benzene resulting in a 40:60 benzene/THF mixture. A prescribed amount of hexamethylcyclotrisiloxane was added to react with the living PEMS anion for 4 h. To avoid broadening of the molecular weight distribution, the PDMS block had to be terminated by trimethylchlorosilane when 50% of the trimer was polymerized.[23] The polymer solution was diluted with THF and washed with distilled water. The block copolymers were precipitated in methanol, filtered off, fractionated from THF solution with methanol in order to remove cyclic monomers and eventually small amounts of homopolymers, and finally dried in vacuo. The total molecular weight was determined by membrane or vapor pressure osmometry, whereas the molecular weight distribution was determined by GPC. ^{1}H NMR analysis was used to determine the molar fraction of PEMS or PDMS respectively. In addition refractive index measurements were used to obtain the weight fraction of PEMS and PDMS. The molecular characteristics of these samples are listed in Table 1. The glass transition temperatures (T_g) measured by differential scanning calorimeter as well as estimates of the ODT temperatures obtained from dynamic shear moduli, G^*, measurements (RMS-800 Rheometrics) are also given in Table 1. Figure 1 shows G' versus temperature for EM-3 and EM-4 samples at frequency 1 rad/s. The observed discontinuity at 250 and 300 K respectively for EM-3 and EM-4 define[24] the ODT. For the latter sample, the kink in the temperature dependence of the depolarized light scattering intensity (inset in FIgure 1) is also characteristic of the ordering transition[25] in good agreement with the ODT estimated from the mechanical measurements.

Photon Correlation Spectroscopy (PCS). The time correlation $G(q,t)$ of the polarized (VV) light scattering intensity at different scattering angles θ (30–150°) was measured with an ALV-5000 full digital correlator covering a wide time range (10^{-6}–10^3 s). The light source was an Ar^+ laser with wavelength λ = 488 nm operating at 150 mW single mode. Both the incident laser beam and scattered light were polarized perpendicular (V) to the scattering plane. Under homodyne conditions, valid for the present system, the measured $G(q,t)$ at a given wave vector $q = (4\pi n/\lambda)\sin(\theta/2)$ (n being the refractive index of the medium) is related to the desired normalized field correlation function $g(q,t)$ by

$$G(q,t) = A_\infty [1 + f^*|\alpha g(q,t)|^2] \quad (10)$$

where f^* is an instrumental factor, α is the fraction of the total polarized scattered intensity $I(q)$ arising from fluctuations in the optical polarizability with correlation times longer than about 10^{-6} s, and A_∞ is the baseline measured at long delay times. The present system exhibits negligibly low depolarized light scattering,[26] and hence, $I(q)$ is virtually the isotropic component of the light scattering intensity due to density and concentration fluctuations with the former being, in principle, much faster. Therefore, the intensity I_c associated with the concentration fluctuations can be estimated from the amplitude α of the experimental correlation function as $I_c(q) = \alpha I(q)$ that defines the absolute Rayleigh ratio $R_c(q) = [I_c(q)/I_T](n/n_T)^2 R_T$ with R_T, I_T, and n_T being the Rayleigh factor of the standard (toluene), its polarized scattering intensity, and its refractive index. $R_c(q)$ is proportional to the static structure factor (eqs 5 and 7) according to

$$R_c(q) = A(n_A^2 - n_B^2)S(q) \quad (11)$$

where the constant $A = v/\lambda^4$. The refractive indices of the two blocks are sufficiently different the amount to[11] 1.427 and 1.403 respectively for PEMS and PDMS at 25 °C.

The characteristic relaxational parameters are routinely extracted by carrying out the inverse Laplace transformation (ILT) of the measured $G(q,t)$ assuming a superposition of exponentials

$$\{[G(q,t)/A_\infty - 1]/f^*\} = \alpha g(q,t) = \int_{-\infty}^{\infty} L(\ln\tau)\exp(-t/\tau)\,d(\ln\tau) \quad (12)$$

At low q's and/or for the low molecular weight EM-1 sample (see below), when the spectrum of the relaxation times $L(\ln\tau)$ is a single peak, the shape of $G(q,t)$ can also be represented by the common Kohlrausch–Williams–Watts (KWW) decay function $g(q,t) = \exp[-(t/\tau)^\beta]$. The distribution parameter β was found to be close to 1 as expected for composition correlation functions at temperatures well above T_g.

IV. Results

Low Molecular Weight. Figure 2 shows experimental net correlations functions $|C(q,t)|^2 = [G(q,t)/A_\infty - 1]/f^*$ at a scattering angle of 30° (q = 0.025 nm^{-1}) for the homogeneous EM-1 diblock at two different temperatures. Since the measurements were performed far above T_g, the dynamics of the density fluctuations due to segmental motion are too fast to be measured by PCS as indicated by the reduced value (less than 1) of the experimental correlation functions at short times. Therefore, these fast density fluctuations do not interfere with the measurements and are not considered here. At 80 °C, $C(q,t)$ appears to be a single decay function whereas at 20 °C there is clearly an additional slow contribution revealed also by the ILT analysis (inset of Figure 2). This slow process, present at low temperatures, is attributed to long-range density fluctuations[27] ("cluster" relaxation). Alternatively, the amplitude α_2 of the main faster process is virtually temperature independent as indicated in the inset of Figure 2. These results of the ILT analysis, eq 12, of the experimental $C(q,t)$ suggest that mainly a single and rather narrow relaxation process describes the dy-

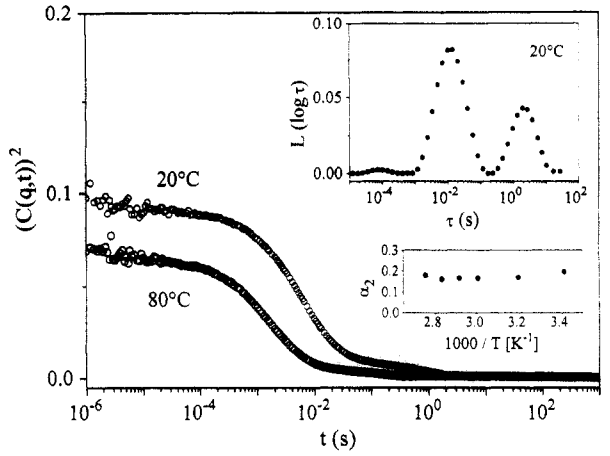

Figure 2. Polarized intensity correlation functions for EM-1 at $q = 0.009$ nm^{-1} ($\theta = 30°$) and temperatures 20 and 80 °C. The inverse Laplace transform of the experimental correlation function at 20 °C and the variation of the amplitude α_2 of the faster process of $C(q,t)$ with temperature are shown in the insets.

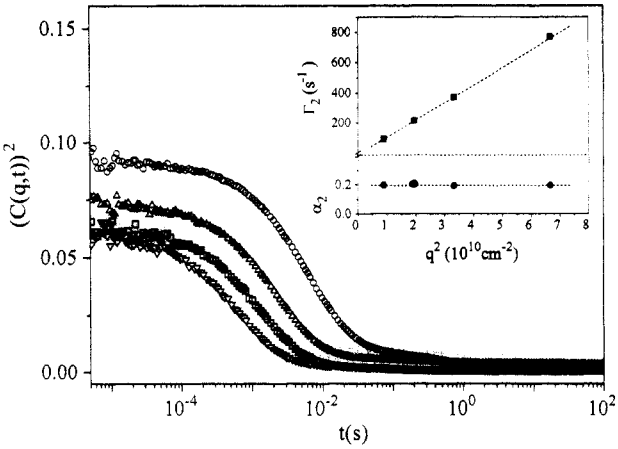

Figure 3. Polarized intensity time correlation functions for EM-1 at 20 °C for different wave vector q's (○, $\theta = 30°$; △, $\theta = 45°$; □, $\theta = 60°$; ▽, $\theta = 90°$). The amplitude α_2 and the relaxation rate Γ_2 of the composition correlation functions are plotted versus the wave vector q in the insets.

namics of composition fluctuations for the low molecular weight EM-1 diblock above 20 °C accounting for about 20% of the total light scattering intensity, $I(q)$. The remaining fraction of $I(q)$ with correlation times faster than 10^{-6} s arises from density fluctuations. In this study, we are interested in the molecular origin of the dynamics of composition fluctuations in diblock copolymer melts above ODT.

The variation of $C(q,t)$ with the probing wavelength $1/q$ is depicted in Figure 3 for EM-1 at 20 °C. The relaxation rate Γ_2 and the amplitude α_2 of $C(q,t)$ obtained from the ILT analysis are shown as a function of the scattering vector q in the insets of Figure 3. The insensitivity of α_2 to q variations is in accordance with short correlation length (ξ) for the composition fluctuations, i.e., $q\xi < 1$, and excludes the possibility of scattering from long-range density fluctuations.[27] Alternatively, the q^2 dependence of Γ_2 is characteristic for diffusive relaxation processes with diffusion coefficient $D = \Gamma_2/q^2$. This process has recently also been observed in two disordered poly(styrene-*block*-methyphenylsiloxane) diblock copolymers[28] and were attributed to either equilibrium composition configurations of the fluctuation theory[15,28] or to the relaxation of the additional composition fluctuations due to the inherent composition polydispersity[13,16] (eq 8). In this context, it is worth mentioning, that the low molecular

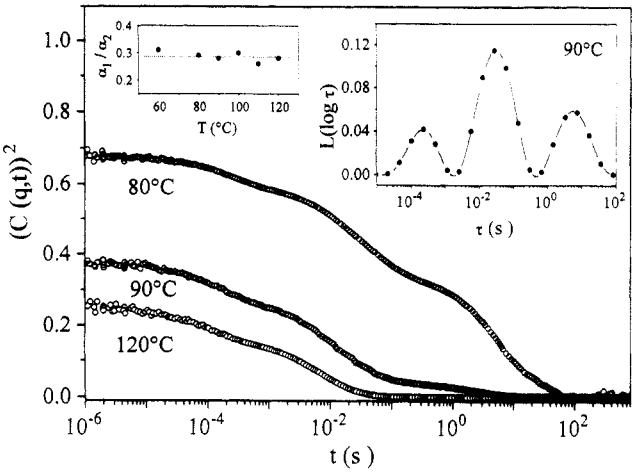

Figure 4. Polarized intensity time correlation functions for EM-4 at $q = 0.025$ nm^{-1} for different temperatures. The inverse Laplace transform (ILT) of the experimental correlation functions at 90 °C and the ratio α_1/α_2 of the amplitudes of the fast internal relaxation to the diffusive mode as a function of temperature are shown in the insets.

weight EM-1 sample is well above ODT, where composition fluctuations are expected to be very weak.

High Molecular Weight. The increase of the molecular weight has a pronounced effect on the dynamics of composition fluctuations in the EM samples above ODT. Figure 4 shows experimental $|C(q,t)|^2$ at $q = 0.025$ nm^{-1} for the highest molecular weight EM-4 diblock at three different temperatures above ODT. Below 120 °C, $C(q,t)$ clearly shows three distinct decays also manifested in the distribution relaxation function $L(\log \tau)$ (inset in Figure 4). The slowest peak of $L(\log \tau)$ loses its amplitude with increasing temperature and, moreover, displays behavior typical of the long-range density fluctuations found in both molecular and macromolecular glass formers.[27] In fact, this slow process (also Figure 2) becomes the dominant contribution to the total intensity $I(q)$ with decreasing temperature and, hence, the two faster relaxations can barely be observed below 60 °C for EM-4. Alternatively, at 120 °C and above, the two fast relaxation modes dominate the composition correlation functions of EM-4 accounting for about 50% of $I(q)$. The ratio α_1/α_2 between the amplitudes of the two relaxation processes obtained from the ILT analysis was found to be virtually insensitive to temperature variations over the examined range (inset in Figure 4). It appears therefore that like α_2 (Figure 2), the amplitude α_1 is also temperature independent.

The variation of the relaxational behavior of $C(q,t)$ with the probing wavelength $1/q$ for EM-4 reflects the nature of the two relaxation modes (eqs 1 and 6). As shown in Figure 5, the relaxation rate of the fast process of $C(q,t)$ appears to be virtually q independent, whereas that of the intermediate decay does depend on q. Note again the increased contribution of the slow "cluster" scattering with decreasing q due to its large correlation length.[26] On the basis of the variation of $L(\log \tau)$ with q and as shown in the inset of Figure 5, the intermediate mode for EM-4 shows a diffusive character similar to the fast process in EM-1 (Figure 3), whereas the rate Γ_1 of the additional fast mode in EM-4 is virtually q independent and is, hence, assigned[9,14] to an internal relaxation of the diblock copolymer chains, i.e., Γ_1 and Γ_2 scale with q^0 and q^2, respectively. The ratio α_1/α_2 between the amplitudes of the two modes is an increasing function of q, and exhibits a q^2 dependence, as shown in the inset of Figure 5. Since α_2 is virtually insensitive to q variations (Figure 3), this dependence is entirely attributed to $\alpha_1(q)$, in agreement

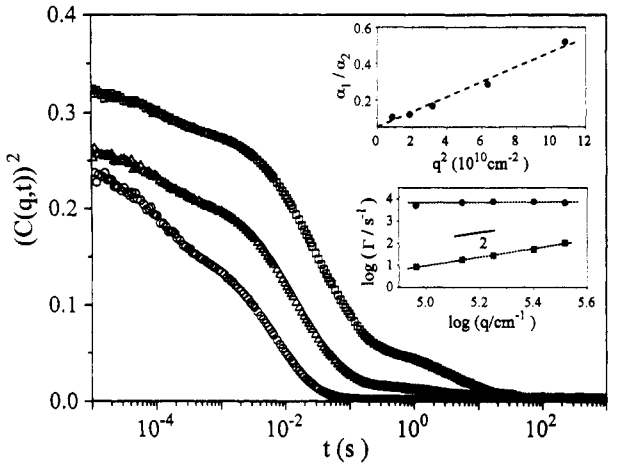

Figure 5. Polarized intensity correlation functions for EM-4 at 120 °C at three scattering angles (□, θ = 45°; △, θ = 60°, ○, θ = 90°). The variation of the relaxation rates of the fast (●) and intermediate (■) processes and of the amplitude ratio α_1/α_2 of the fast internal relaxation to the diffusive process with q is shown in the insets. The solid line in the inset indicates a slope of 2.

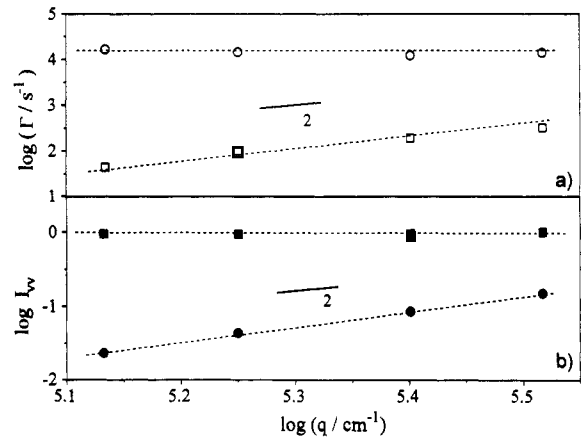

Figure 6. Wave vector dependence of (a) the relaxation rates for the fast internal relaxation and the intermediate diffusive process and (b) the dynamic intensities associated with the two processes for EM-3 at 120 °C. The solid lines indicate a slope of 2. Circles represent the fast internal relaxation, whereas squares denote the intermediate diffusive mode.

with the prediction for $S_1(q)$ of eq 5. Figure 6a shows the variation of the relaxation rates Γ_1 and Γ_2 of the internal relaxation and the diffusive mode with scattering wave vector q for sample EM-3 at 120 °C. Similar to EM-4, Γ_2 clearly shows a diffusive character (q^2-dependent rate), whereas the fast rate Γ_1 is virtually q independent. The corresponding intensities $I_1(q) = \alpha_1 I(q)$ and $I_2(q) = \alpha_2 I(q)$ for the two processes in EM-3 display different q dependencies as shown in Figure 6b. While the intensity I_2 associated with the diffusive process is virtually q independent (see also inset of Figure 3), $I_1(q)$ exhibits a strong ($\sim q^2$) dependence on q. This is in agreement with the amplitude ratio α_1/α_2 for EM-4 in the inset of Figure 5 found to vary linearly with q^2. Finally, the absence of the internal mode in the low molecular weight EM-1 sample (Figure 2) can be attributed[14] to its low amplitude, as will be discussed in section V.

Summarizing the experimental findings, the dynamics of the composition fluctuations in disordered diblock copolymer melts display bimodal relaxational behavior. The fast relaxation is characterized by q-independent relaxation rate but its amplitude is almost q^2 dependent and increases with molecular weight. Alternatively, the second slower relaxation has a diffusive nature (q^2-dependent rate) with the associated scattering intensity being virtually q independent. The relaxation rates of both processes depend on the molecular weight, to be discussed in relation to Figure 8 below. The results will be discussed below in conjunction to the theoretical predictions of section II.

Table 2. Static Structure Factor from Composition Polydispersity

sample	T (°C)	χN	R_ρ (10^{-5} cm^{-1})	R_{VV} (10^{-5} cm^{-1})	R_2 (10^{-5} cm^{-1})	$S_2(q)$	κ_o
EM-1	80	1.5	2.1[a]	2.6	0.46	2.9	$1.2\cdot10^{-2}$
EM-2	80	3.5	2.1[a]	2.8	0.74	4.7	$0.8\cdot10^{-2}$
EM-3	120	4.7	2.5	5.8	3.0	17.4	$1.7\cdot10^{-2}$
EM-4	120	6.3	2.5	4.9	1.84	10.5	$0.8\cdot10^{-2}$
EM-5	80	4.9	2.1[a]	5.9	3.4	19.5	$1.8\cdot10^{-2}$

[a] Estimated from homopolymer data.[11]

V. Discussion

Diffusive Relaxation. All samples of Table 1 display dynamic light scattering arising from long wavelength composition fluctuations irrespective of the proximity of the ODT. Relaxation of composition field configurations (pattern) with a correlation length ξ recently employed to discuss the diffusive process in poly(styrene-*block*-methylphenylsiloxane) diblock copolymers[15,28] is not very likely far above ODT. Instead, the origin of the diffusive process is the presence of composition polydispersity in diblock copolymer systems inducing significant composition fluctuations at low q's. We will therefore discuss the results of the EM samples in terms of the theoretical predictions of eqs 6–9.

For EM-1, only the diffusive process contributes to $C(q,t)$ (Figure 2) and the associated state structure factor $S_2(q)$ computed from eq 11 is listed in Table 2 along with the total absolute intensity, R_{VV}, and the contribution of the density fluctuations, R_ρ. The latter is quite close to an average of the light scattering intensities arising from the two homopolymers. For the other two samples EM-3 and EM-4, one part, $R_2(q)$, of the light scattering intensity $I_c(q)$ is due to the diffusive process and another, $R_1(q)$, to the internal relaxation of the copolymer chain. The low molecular weight EM-1 sample displays only about 20% more light scattering intensity than the bulk hompolymers. On the other hand, the high molecular weight EM-4 sample scatters more than twice as much light at low q's as the constituent homopolymers. On the basis of eq 7, this disparity arises from sufficient composition polydispersity as well as large enough molecular weight. The estimated from $S_2(q)$ and eq 7 values for κ_o, describing the former, is also listed in Table 2. Apparently, there is a relation between the values of κ_o and the degree of polydispersity M_2/M_n (Table 1) in these samples. The quantity $2\chi N\kappa_o$ in the denominator of eq 7 is significantly smaller than 1 and hence, unlikely the situation in blends, $S_2(q)$ is not very sensitive to the proximity of ODT for anionically synthesized diblocks; at ODT, $S_2(q)$ could increase up to 50%. In fact, the amplitude α_2 of the diffusive relaxation is virtually insensitive to temperature variations (inset of Figure 2). Similar behavior is also observed for the temperature dependence of the diffusion coefficient D.

For the composition polydispersity mode, D is given by eq 8, that can be rewritten as:

$$D = D_s(N)\,\kappa_o v N/S_2(q) \qquad (13)$$

Since $S_2(q) \cong \kappa_o N$ (Table 2), D should display very similar temperature dependence with that of the copolymer chain diffusion. The temperature dependence of the latter is

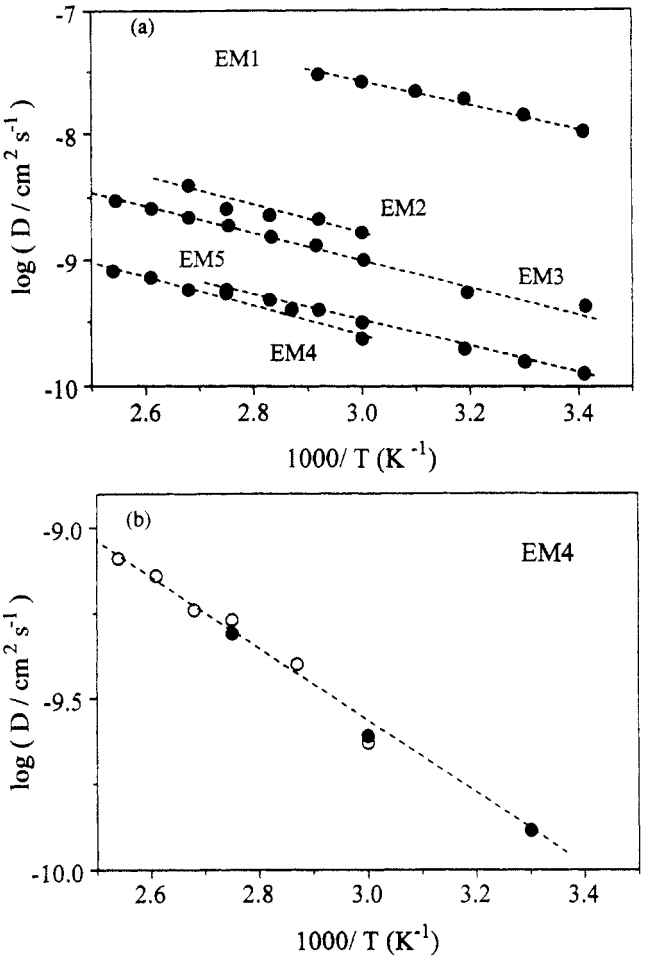

Figure 7. Arrhenius plot of the diffusion coefficient D of the composition polydispersity process for five EM samples (a). The comparison between D (○) and self-diffusion D_s (●) for the EM-4 copolymer chain obtained from pulsed-field gradient NMR is illustrated in b.

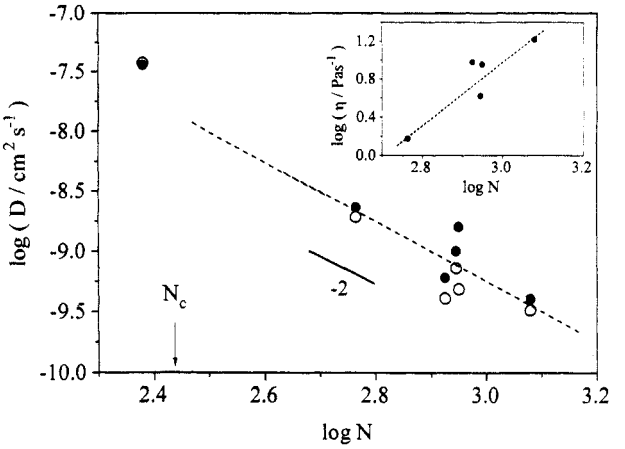

Figure 8. The variation of the diffusion coefficient D with the degree of polymerization N for six EM samples at 80 °C. Solid and open symbols denote respectively experimental and computed (eqs 9 and 13) diffusion coefficients. N_c stands for the entanglement limit; the slope −2 is the reptation prediction (eq 9b), and the dashed line is a guide to the eye. The experimental zero shear viscosities as a function of N for the five entangled samples at 80 °C is shown in the inset, where the line is a fit to the data for the symmetric diblocks.

determined by the variation of the microscopic friction ζ_o with temperature and is expected to be the same in all samples having effectively the same T_g. Figure 7a shows an Arrhenius plot of D for the five EM copolymers. As expected for temperatures far above T_g, all samples exhibit an Arrhenius dependence with an activation energy E_D = 4.8 ± 0.4 kcal/mol being very close to the average activation energy (4.9 kcal/mol) obtained from viscosity measurements on the two homopolymers.[22] The data of Figure 7a are therefore in agreement with a temperature-independent static structure factor $S_2(q) \cong \varkappa_o N$ and, hence, imply that D in eq 6 is essentially the chain self-diffusion D_s. Note that this is true for relatively small values of the variance of the composition polydispersity, $\varkappa_o$. Figure 7b illustrates the comparison between D as measured by PCS and D_s as obtained from pulse-field gradient nuclear magnetic resonance (NMR) measurements on the EM-4 copolymer. In the overlapping temperature range, the observed agreement strongly supports the prediction of eqs 8 and 13 which can now be used to compute D for the other EM samples.

For the entangled EM-2, EM-3, and EM-5 copolymers, eq 9b can yield the value of D_s using[22,14] N_e = 125 and the microscopic friction ζ_o of EM-4 computed from eq 9a and the self-diffusion data of Figure 7b. The comparison between the experimental (solid symbols) and the calculated (open symbols) diffusion coefficients at 80 °C is visualized in Figure 8 as a function of the total molecular weight of the diblocks. This isothermal plot becomes feasible for the present model diblock copolymer since T_g effects equally affect all samples due to the very low and similar T_g's of the two components. The data for the five entangled samples conform to the N^{-2} dependence, as expected for self-diffusion.[18] The computation assumes the validity of the reptation eq 9b for all samples but EM-1. In fact, the zero shear viscosity data for the same diblocks (inset of Figure 8) exhibit a close to the well-known $N^{3.4}$ dependence. The deviation between computed and experimental diffusion coefficients amounts to about 20% for EM-2 and EM-5 and 60% for EM-3 which possesses relatively high polydispersity (Table 1) and asymmetric distribution.[29] The presence of copolymer chains with low molecular weight can increase the mobility and lead to enhanced diffusivity D. For the low molecular weight unentangled EM-1, the estimated D_s using the Rouse expression of eq 9a, with $\zeta_o = 5 \times 10^{-9}$ g s^{-1} (at 80 °C) obtained from shear mechanical data of the homopolymers,[29] approach the experimental D within 10%. As expected, this sample exhibits faster chain diffusivity than the extrapolated value based on the reptation eq 9b. The diffusive relaxation process in disordered EM copolymer melts can, therefore, be rationalized in terms of composition polydispersity effects and is essentially envisaged as copolymer chain self-diffusion being rather insensitive to thermodynamic interactions, eqs 8 and 13.

We have recently reported[28] on the diffusive process in poly(styrene-*block*-methylphenylsiloxane) (SM) diblock copolymer melts near and above ODT. In contrast to the EM copolymers in this manuscript, the two homopolymer blocks possess vastly different segmental mobilities which might affect the comparison between theory and experiment. Figure 9 shows an Arrhenius plot of the experimental diffusion coefficients (solid points) in SM-1 (N = 99, w_S = 0.49, M_w/M_n = 1.12) and SM-2 (N = 277, w_S = 0.27, M_w/M_n = 1.14). Note the different temperature dependencies of the experimental D for the two samples due to the different effective T_g's. The variation of D for the two SM samples with temperature, resembles that of the self-diffusion of bulk polystyrene (PS) homopolymer, also shown in Figure 9. In RPA calculations, it is the higher friction coefficient of PS-rich environment that dominates the diffusional dynamics. The computed values (open symbols) were obtained from eq 9a using friction coefficients derived from experimental viscosity η data, ζ_o

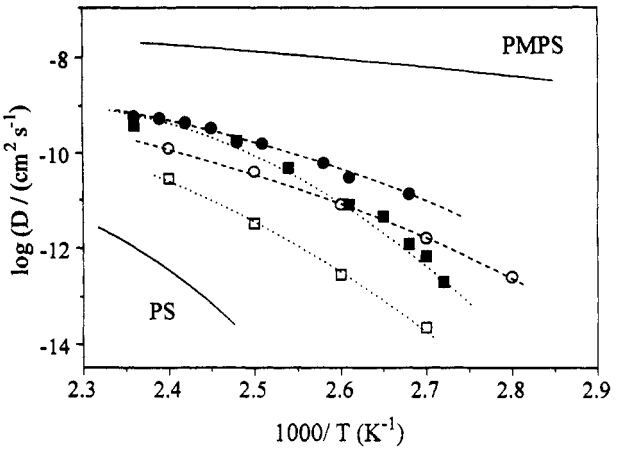

Figure 9. Arrhenius plot of the diffusion coefficient D (solid points) for two poly(styrene-*block*-methylphenylsiloxane) copolymers[28] (●, SM-1, ■, SM-2 of ref 28). The two solid lines denote the self-diffusion coefficients D_s for the two homopolymers (M_n = 21 000). The open symbols denote calculated diffusivities based on eq 9a.

$= 36\eta v/Nb^2$. Although the temperature dependencies of the computed and experimental D are essentially the same, the calculation (eq 9a) underestimates the measured D. The difference amounts to a factor of 4 and 20 respectively for SM-1 and SM-2. For the latter, probably weakly entangled, an even larger deviation should result if the reptation expressions of η and D (eq 9b) were used. In contrast to the situation in Figure 8, the disagreement in Figure 9 might arise from the large difference between segmental frictions. Equation 8 was derived for polydisperse copolymer chains with blocks possessing the same local friction. The fact however, that the underestimation of the experimental D becomes severe with increasing N can signal the importance of the composition fluctuations with their amplitude being larger in SM-2. At present it is not clear, however, why η ($\sim\zeta_0$) is more amenable to the composition fluctuation effects[24] than D_s[30] and, apparently, D.

Internal Diblock Relaxation. The composition fluctuations in monodisperse A–B copolymers arise from the relative translational motion of the two blocks and the RPA predictions for the thermal decay rate $\Gamma_1(q)$ and the static structure factor $S_1(q)$ are respectively given by eqs 4 and 5. These equations are also valid in the presence of small composition polydispersity.[13,16] We will discuss the fast relaxation process in EM (Figures 4–6) in terms of this internal copolymer chain motion.

The variation of the experimental relaxation rates Γ_1 with temperature and total degree of polymerization N is shown in Figure 10. The Arrhenius activation energy of Γ_1 is experimentally the same with that of chain diffusion D (Figure 8), in accordance with eqs 4 and 9 in the absence of thermodynamic effects at low wave vectors. In this limit, substitution of eq 5 into eq 4 for entangled chains leads to the thermal decay rate[14]

$$\Gamma_1 = \frac{36}{5f(1-f)}\frac{k_B T}{\zeta_0 b^2}\frac{N_e}{N^3} \qquad (14)$$

where the microscopic friction ζ_0 dictates the temperature dependence of Γ_1. The low q limit is approached by the present EM copolymers since, even for the highest molecular weight diblock, the largest $x = q^2 R_g^2 \cong 0.1$. It should also be mentioned that eq 14 is derived from eq 4, where a particular choice of the Onsager coefficient has been made.[31] An alternative expression, derived for

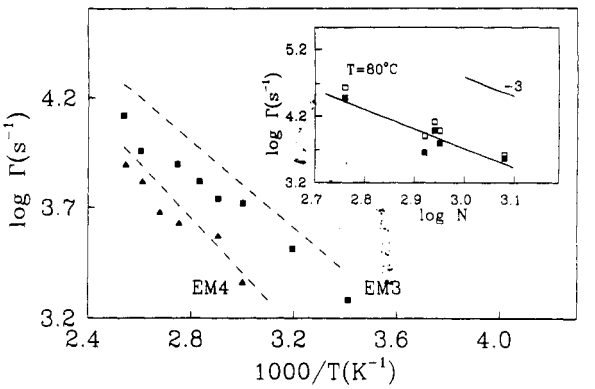

Figure 10. Arrhenius plot of the thermal decay rate Γ_1 for two EM samples. The solid points and the dashed lines denote respectively experimental and calculated (eq 14) values. The inset shows the variation of experimental (solid symbols) and calculated (open symbols) Γ_1 at 80 °C with the total degree of polymerization N. The line shows the predicted −3 slope (eq 14).

entangled copolymers,[31c] leads to the same result for the symmetric case (f = 1/2). On the other hand, strong thermodynamic effects are predicted[9,17] to be absent for $x \ll x^*$. The present diblock copolymer system is suitable for such a study in the disordered state, on account of its relatively low Arrhenius activation energy and small interaction parameter;[29] the synthesis of adequately very high molecular weight copolymers ($\sim 10^6$) are in progress.

In the low q range, Γ_1 can be computed from eq 14 with $\zeta_0 = 370\eta v N_e^{2.5}/(b^2 N^{3.5})$, derived from zero shear viscosity η (= $\lim_{\omega\to 0} G''(\omega)/\omega$) measurements (inset of Figure 8); the expression for ζ_0 is valid for homopolymers.[11] The calculated Γ_1's are also shown in Figure 10 with dashed lines. For the symmetric EM-3 and EM-4 diblocks, the theoretical values exceed the experimental Γ_1, respectively, by about 25% and 15% whereas for the asymmetric EM-5 (not included in Figure 10) this disparity increases to about 35%. While the reptation expressions for both Γ_1 and η are expected to apply at very high molecular weights, it is the product $\Gamma_1\eta$ ($\sim N^{0.5}$) that enters in eq 14. Hence, the overall reasonable agreement of eq 14 with experimental Γ_1 cannot be considered as a crucial verification of the reptation relations. The systematic deviation between computed and experimental Γ_1 values in the Arrhenius plot of Figure 10 can be attributed to uncertainties in the value of some quantities (e.g., N_e, N), to the exactness of the expression for the viscosity and eq 14, as well as to the determination of the average τ, eq 12, although the distribution $L(\log \tau)$ is quite narrow. Furthermore, the increased disparity between theoretical and experimental Γ_1 in the asymmetric EM-5 (f_E = 0.7) rich in PEMS mimics the concentration dependence of the friction coefficient which is larger in PEMS than in PDMS homopolymer;[11,22] Γ_1 is also a decreasing function of f_E at constant N (inset in Figure 10).

According to eq 14, the thermal decay rate of the composition fluctuations should scale with N^{-3}. Experimental and computed Γ_1 at 80 °C are shown as a function of N in the inset of Figure 10. The experimental points for the symmetric EM diblocks yield $D \approx N^{-(2.9\pm0.1)}$, whereas inclusion of Γ_1 for EM-5 and EM-6 leads to the somewhat lower exponent −2.8. Alternatively, the computed Γ_1 (empty symbols in the inset of Figure 10) of the symmetric samples conform to a scaling relation with exponent −3.2 that is slightly larger than the reptation prediction of eq 14, due to the strong molecular weight dependence of the viscosity ($N^{3.4}$, inset of Figure 8). Inclusion of the asymmetric samples has negligible effect on the value of the scaling exponent. It is apparent from the data in the

Table 3. Static Structure Factor for the Internal Chain Relaxation at 120 °C and q = 0.025 nm^{-1}

sample	f_E[a]	qR_g	$R_q(q)$ (10^{-5} cm^{-1})	$S_1(q)_{exp}$	$S_1(q)_{theo}$
EM-3	0.46	0.19	0.30	1.7	1.4
EM-4	0.51	0.22	0.53	3.0	2.5
EM-5	0.70	0.19	0.35	2.0	0.9

[a] Volume fraction of polyethylmethylsiloxane block, PEMS.

inset of Figure 10 that the experimental Γ_1 systematically decreases with increasing PEMS composition at constant N (samples EM-6 to EM-3 to EM-5) that also follows the composition dependence of ζ_o (Figure 3, ref 11). It is worth mentioning that this variation is less pronounced in the computed Γ_1, i.e., in the viscosity. Nevertheless, the dynamics of the fast relaxation process in EM can adequately be described by the RPA and reptation predictions.

The static structure factor $S_1(q)$ associated with the internal relaxation can be obtained from the amplitude α_1 of the experimental $C(q,t)$, the total light scattering intensity $I(q)$ and eq 11. Alternatively, eq 5 is the RPA theoretical prediction for $S_1(q\to 0)$ at low q's. For two symmetric and one asymmetric EM copolymer, the values are listed in Table 3 along with the experimental absolute Rayleigh ratio $R_1(q)$ for q = 0.025 nm^{-1} and 120 °C. The contribution R_ρ of the density fluctuations to the total R_{VV} was estimated for EM-3 and EM-4 and assumed to be the same in the EM-5 sample. $S_1(q)_{theo}$ was computed from eq 5 using b = 6.3 Å, whereas $S_1(q)_{exp}$ was estimated from the experimental $R_1(q)$ using $(n_A^2 - n_B^2) = 9.4 \times 10^{-4}$ at 120 °C for all samples. The values of these parameters at high temperatures are additional sources of errors in the derivation of either structure factor with an uncertainty of about 10%. For EM-4 and EM-3, the difference of about 16% between the two values of $S_1(q)$ listed in Table 3 is therefore not significant. This however, cannot be claimed for the asymmetric EM-5 for which the experimental structure factor is about twice the computed $S_1(q)_{theo}$. To circumvent the necessity of using absolute intensities, we compared the ratio between the values of $S_1(q)_{theo}$ in two samples with the corresponding ratio of $S_1(q)_{exp}$. For EM-4 and EM-3, the theoretical $[S_1(q)_{theo}]_{EM\text{-}4}/[S_1(q)_{theo}]_{EM\text{-}3} = 1.8$ almost coincides with the value of the corresponding experimental ratio. On the contrary, while the theory predicts significantly stronger internal relaxation in EM-3 than in EM-5 ($[S_1(q)_{theo}]_{EM\text{-}3}/[S_1(q)_{theo}]_{EM\text{-}5} = 1.5$) the experimental finding is that $[S_1(q)_{exp}]_{EM\text{-}3}$ is slightly less than $[S_1(q)_{exp}]_{EM\text{-}5}$. At present the latter disparity can be attributed to the composition dependence of $S_1(q)$ in eq 5.

The internal chain relaxation was experimentally observed when $qR_g \geq 0.1$ and its amplitude was found to increase with q (Figures 5 and 6). According to eq 5, $S_1(q)$ should scale with q^2, i.e., the light scattering intensity increases with decreasing the probing wavelength. Figure 6b shows the variations of the absolute Rayleigh ratio $R_1(q)$ with the magnitude of the scattering wave vector for EM-3 and EM-4 at 120 °C. The experimental data of Figure 6b conforms well to a q^n law with $n = 2 \pm 0.2$, thus verifying the q^2 dependence of eq 5. As anticipated from eq 5, this variation is virtually independent of temperature.

It is evident from the intensities of Tables 2 and 3 that the experimental "polydispersity" diffusive mode dominates the composition correlation functions (Figures 4 and 5). According to eqs 5 and 7, the ratio of the structure factors associated with the two relaxation processes for low wave vectors is given by

$$\frac{S_1(q)}{S_2(q)} \to \frac{2}{3}[f(1-f)qR_g]^2[1 - 2\chi N \varkappa_o] \qquad (15)$$

For the symmetric samples EM-3 and EM-4 at 120 °C and q = 0.025 nm^{-1} the computed ratio $S_2(q)/S_1(q)$ amount to 11 and 4, respectively. The experimental R_2/R_1 for EM-3 and EM-4 is respectively 10 and 3.5 in agreement with the computed values. However, for the asymmetric EM-5 the agreement is again less satisfactory.

VI. Concluding Remarks

Diblock copolymer melts above ODT display significant dynamic light scattering arising from fast density and composition fluctuations. For the present EM copolymers, the former have correlation times faster than 10^{-7} s and account for about 50% of the total light scattering intensity at low q's. Alternatively, the dynamics of composition fluctuations as studied by photon correlation spectroscopy reveal two distinct relaxation processes, besides the slow long-range density fluctuations, which exhibit different pertinent features. The intermediate and fast relaxation modes are identified, respectively, with the interdiffusion of the copolymer chains, becoming observable through the inherent composition polydispersity, and the internal copolymer chain relaxation via the relative translational motion of the two blocks. These are the main mechanisms causing thermal composition fluctuations in homogeneous copolymer melts.

The structure factor associated with the slow diffusive process is related to the composition polydispersity of the samples, whereas the diffusion coefficient is essentially the self-diffusion of the copolymer chains. For the EM copolymers consisting of two blocks with similar segmental mobilities, the experimental diffusion coefficient, D, agrees well with the copolymer self-diffusion coefficient D_s, either measured by pulsed-field gradient NMR or calculated using frictions estimated from shear viscosity data. However, for the poly(styrene-*block*-methylphenylsiloxane) diblocks with components possessing vastly different segmental mobilities, the agreement between D and D_s estimated using viscosity data is found to be rather poor.

For the internal relaxation mode, the RPA predictions for the static structure factor $S_1(q)$ and thermal decay rate Γ_1 at low q's are experimentally verified. This process observed in EM samples when $qR_g \geq 0.1$ has a q^2-dependent amplitude whereas Γ_1 is insensitive to q variation but exhibits a strong dependence ($\sim N^{-3}$) on the total degree of polymerization N. Besides to the conformity to the theoretical scaling laws, the RPA predictions in the low q limit (eqs 5 and 14) can quantitatively predict the experimental $S_1(q)$ and Γ_1 for the symmetric EM samples. For the present EM's the highest qR_g value is about 0.3, i.e., $x \cong 0.1$ and, hence, both $S_1(q)$ and Γ_1 show no evidence of thermodynamic effects. Experimental verification of the latter as well as the q dependence of Γ_1 requires high x values of the $O(x^*)$.

Acknowledgment. The financial support of the Alexander von Humboldt Foundation (grant no. FOKOOP USS 1685) is gratefully acknowledged. G.F. appreciates financial support from the Max Planck Society and the warm hospitality of Max-Planck-Institut für Polymerforschung in Mainz. S.H.A. would like to acknowledge that part of this research was sponsored by NATO's Scientific Affairs Division in the framework of the Science for Stability Programme and by the Greek General Secretariat of Research and Technology. We thank Prof. A. N. Semenov for stimulating discussions and Dr. G.

Fleischer for the pulsed-field gradient Nuclear Magnetic Resonance measurements.

References and Notes

(1) Fytas, G.; Anastasiadis, S. H. In *Disorder Effects on Relaxation Processes*; Richert, R., Blumen, A., Eds.; Springer Verlag: Berlin, 1994.
(2) Bates, F. S.; Fredrickson, G. H. *Annu. Rev. Phys. Chem.* **1990**, *41*, 525.
(3) Helfand, E.; Wasserman, Z. R. In *Development of Block Copolymers I*; Goodman, I., Ed.; Applied Science: London, 1982.
(4) Fried, H.; Binder, K. *J. Chem. Phys.* **1991**, *94*, 8349. Gauger, A.; Weyesberg, T.; Pakula, T. *Makromol. Chem., Theory Simul.* **1993**, *2*, 531.
(5) Jian, T.; Anastasiadis, S. H.; Semenov, A. N.; Fytas, G.; Yeh, F. J.; Chu, B.; Vogt, S.; Wang, F.; Roovers, J. E. L. *J. Chem. Phys.* **1994**, *100*, 3286.
(6) Karatasos, K.; Anastasiadis, S. H.; Fytas, G.; Pispas, A.; Hadjichristidis, N.; Roovers, J. E. L.; Pakula, T. *Macromolecules* **1994**, submitted for publication.
(7) Leibler, L. *Macromolecules* **1980**, *13*, 1602.
(8) Fredrickson, G. H.; Helfand, E. *J. Chem. Phys.* **1987**, *87*, 697. Barrat, G. L.; Fredrickson, G. H. *J. Chem. Phys.* **1991**, *95*, 1282.
(9) Akcasu, A. Z.; Benmouna, M.; Benoit, H. *Polymer* **1986**, *27*, 1935. Akcasu, A. Z.; Tombakoglu, M. *Macromolecules* **1990**, *23*, 607. Akcasu, A. Z. *Macromolecules* **1991**, *24*, 2109.
(10) Borsali, R.; Vilgis, T. A. *J. Chem. Phys.* **1990**, *93*, 3610.
(11) Meier, G.; Fytas, G.; Momper, B.; Fleischer, G. *Macromolecules* **1993**, *26*, 5310, and references therein.
(12) Borsali, R.; Fischer, E. W.; Benmouna, M. *Phys. Rev. A* **1993**, *43*, 5732. Borsali, R.; Benoit, H.; Legrand, J.; Duval, M.; Picot, C.; Benmouna, M.; Farago, B. *Macromolecules* **1989**, *22*, 4115.
(13) Jian, T.; Anastasiadis, S. H.; Semenov, A. N.; Fytas, G.; Adachi, K.; Kotaka, T. *Macromolecules* **1994**, submitted for publication.
(14) Anastasiadis, S. H.; Fytas, G.; Vogt, S.; Fischer, E. W. *Phys. Rev. Lett.* **1993**, *70*, 2415.
(15) Anastasiadis, S. H.; Fytas, G.; Vogt, S.; Gerharz, B.; Fischer, E. W. *Europhys. Lett.* **1993**, *26*, 619.
(16) Fytas, G.; Anastasiadis, S. H.; Semenov, A. N. *Makromol. Chem., Macromol. Symp.* **1994**, *79*, 117. Semenov, A. N.; Fytas, G.; Anastasiadis, S. H. *Polym. Prepr.* **1994**, *35* (1), 618.
(17) Fredrickson, G. H.; Larson, R. G. *J. Chem. Phys.* **1987**, *86*, 1553.
(18) Doi, M.; Edwards, S. F. *The Theory of Polymer Dynamics*; Oxford Science Publ.: Oxford, 1986.
(19) Fytas, G. *Macromolecules* **1987**, *20*, 1430. Green, P. F.; Doyle, B. L. *Macromolecules* **1987**, *20*, 2471.
(20) Jian, T. Ph. D. Dissertation, University of Athens, Athens, Greece, 1994.
(21) Momper, B.; Wagner, Th.; Maschke, U.; Ballauff, M.; Fischer, E. W. *Polym. Commun.* **1990**, *31*, 187.
(22) Momper, B. Ph. D. Dissertation, University of Mainz, Mainz, Germany, 1989.
(23) Morawetz, H.; Cho, J. R.; Gans, P. S. *Macromolecules* **1973**, *6*, 624. Wilczek, L.; Kennedy, I. P. *Polym. J.* **1987**, *19*, 531. Maschke, U. Ph. D. Dissertation, University of Mainz, Mainz, Germany, 1992.
(24) Rosedale, J. H.; Bates, F. S. *Macromolecules* **1990**, *23*, 2329.
(25) Jian, T.; Anastasiadis, S. H.; Fytas, G.; Adachi, K.; Kotaka, T. *Macromolecules* **1993**, *26*, 4706.
(26) Fytas, G.; Patkowski, A.; Meier, G.; Fischer, E. W. *Macromolecules* **1988**, *21*, 3250.
(27) Fischer, E. W. *Physica A* **1993**, *201*, 183. Gerharz, B.; Meier, G.; Fischer, E. W. *J. Chem. Phys.* **1990**, *92*, 7110.
(28) Vogt, S.; Jian, T.; Anastasiadis, S. H.; Fytas, Fischer, E. W. *Macromolecules* **1993**, *26*, 33.
(29) Vogt, S. Ph. D. Dissertation, University of Mainz, Mainz, Germany, 1993.
(30) Shull, K. R.; Kramer, E. J.; Bates, F. S.; Rosedale, J. H. *Macromolecules* **1991**, *24*, 1383. Balsara, N. D.; Stepanek, P.; Lodge, T. P.; Tirrell, M. *Macromolecules* **1991**, *24*, 6227. Ehlich, D.; Takenaha, M.; Okamoto, S.; Hashimoto, T. *Macromolecules* **1993**, *26*, 189.
(31) Pincus, P. *J. Chem. Phys.* **1981**, *75*, 1996. Binder, K. *J. Chem. Phys.* **1983**, *79*, 6387. Kawasaki, K.; Sekimoto, K. *Macromolecules* **1989**, *22*, 3063.